Field emission properties of edge-functionalized graphene

Yanlin Gao*, Susumu Okada

Graduate School of Pure and Applied Sciences, University of Tsukuba, 1-1-1 tennodai, Tsukuba 305-8571, Japan

Abstract

A comprehensive study on electrostatic potential properties of edge-functionalized graphene under an external electric field was performed by using the density functional theory. The shapes and attached functional groups of the edges cause substantial variation of their electrostatic potential outside the edges.Our calculations reveal that graphene edges functionalized by H, OH, and COOH cause relatively large emission current for a wide range of the electric field due to the decrease in the potential barriers caused by the dipoles compared to that before functionalization, while an O termination substantially suppresses the current by increasing the potential barrier. In addition, the NH group increases and decreases the field emission current of graphene with zigzag and armchair edges, respectively, because of the different electrostatic environment around the edge atomic sites arising from the NH group conformations at the edges.

1. Introduction

A hexagonal covalent network of sp^2 C atoms endows graphene with unusual mechanical and electronic properties. The tightly bound electrons in its covalent bonds cause the remarkable stability and mechanical stiffness, allowing graphene to be a constituent material of thermal and thermoelectric devices. The π electron network causes pairs of linear dispersion bands at the six corners

*Corresponding author
Email address: ylgao@comas.frsc.tsukuba.ac.jp (Yanlin Gao)

of the hexagonal Brillouin zone, giving graphene a remarkable carrier mobility of up to 200000 $cm^2V^{-1}s^{-1}$ [1, 2, 3]. Because of its high aspect ratio, mechanical stiffness, chemical stability, and excellent conductivity, graphene is a promising material for field emission devices. Electron emissions from graphene-based materials have been studied extensively [4, 5, 6, 7, 8, 9]. Electron emission of graphene has been experimentally found to occur mainly at its edge atomic sites [6, 7]. Furthermore, the turn-on electric field for electron emission is improved by coating with a metal oxide [8]. In addition, field emission properties of graphene and graphene-related materials depend on the growth condition and substrate species, which seriously affect their local and global structures. Graphene synthesized on a titanium substrate at high H_2 gas concentration shows a remarkable field enhancement factor of up to 7500 [9]. Several microscopic simulations on graphene with zigzag and armchair edges have revealed that the edges enhance the field emission properties of graphene and its derivatives [10, 11, 12, 13, 14].

In practical field emission devices, graphene may have structurally rough edges terminated by various functional groups. These edge variations cause its versatile electronic structures. For example, theoretical calculations predicts that graphene nanoribbons (GNRs) with amchair edges are either metals or semiconductors depending on the GNR width [15, 16, 17], while graphene with hydrogenated zigzag edges has peculiar edge-localized non-bonding states, causing spin polarization at the edge atomic sites [15, 16, 18, 19]. Following the theoretical prediction, the edge-localized state has been observed using a scanning tunneling microscope [19, 20, 21, 22, 23, 24]. In addition, graphene with hydroxylated zigzag edges is a metal with delocalized states possessing nearly free electron (NFE) nature in the vacuum spacing and alongside the edges together with the edge states [25, 26, 27, 28, 29]. These facts imply that the field emission properties of graphene strongly depend not only on the edge shape but also on the edge functionalization.

Although experiments on graphene field emission have steadily advanced, the effect of edge functionalization on this emission is still unclear. Therefore, in this

work, we aim to clarify the field emission properties of graphene edges in terms of their attached functional groups. Using the density functional theory (DFT) combined with the effective screening medium (ESM) method, we investigated the electrostatic potential properties of GNRs with armchair and zigzag edges functionalized by O, CHO, COOH, H, NH, and OH groups under an external electric field. Our calculations show that the electrostatic potential properties of these GNRs depend on the functional groups. Accordingly, the emission current depends not only on the applied electric field but also on the functional groups. GNRs with H, OH, and COOH functionalized edges exhibit remarkable field emission current from their edges, owing to the small potential barrier outside their edges. In contrast, the edges with the O termination result in a low emission current compared with other functionalized edges, owing to the large electrostatic potential barrier outside the edges.

2. Calculation methods

All calculations in this study were based on DFT [30, 31] implemented in the Simulation Tool for Atom TEchnology (STATE) package [32]. The exchange-correlation potential among interacting electrons was treated using the generalized gradient approximation with the Perdew-Burke-Ernzerhof functional [33]. The interaction between electrons and ions was described by ultrasoft pseudopotentials generated by the Vanderbilt scheme [34]. The valence wave function and deficit charge densities were expanded in terms of plane-wave basis sets with cut-off energies of 25 and 225 Ry, respectively. All atomic structures were optimized until the force on each atom was below 5 mRy/Å under the zero-electric-field condition. Integration over the Brillouin zone was carried out using equidistant 4-k points in one-dimensional Brillouin zone along ribbon direction, which enabled sufficient convergence in the total energy and electronic structures of graphene and other carbon materials [16]. All atomic structures were fixed as those under zero-electric field during the calculations of electronic properties under an external electric field.

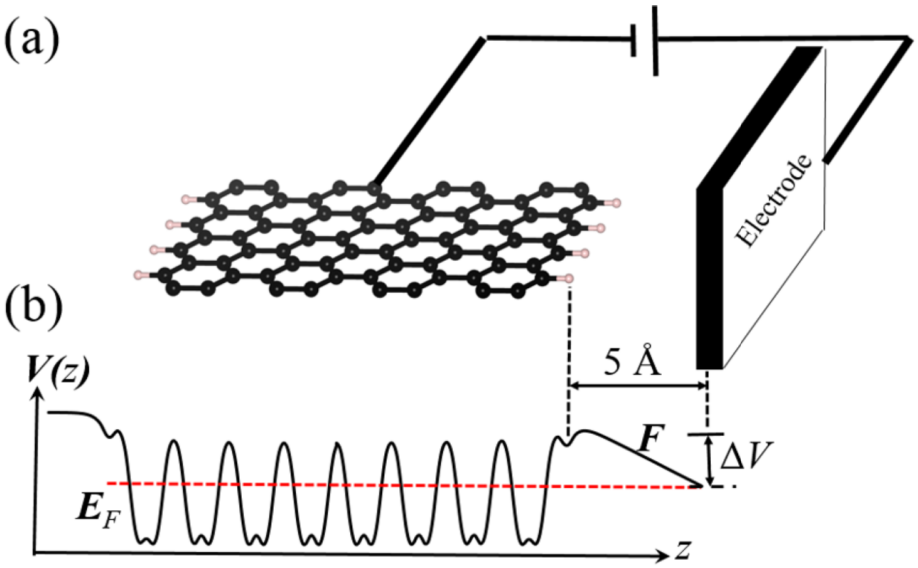

Figure 1: (a) Structural model and (b) schematic diagram of the plane-averaged electrostatic potential of a GNR under a lateral electric field. The dashed horizontal line is the Fermi energy, and ΔV denotes the electrostatic potential barrier for electron emission from the edges.

The ESM method was used to investigate the electrostatic potential properties of edge-functionalized GNRs under a lateral electric field. To apply an electric field to the graphene edge, we considered a planar counter metal electrode described by an ESM with an infinite relative permittivity and separated by 5 Å vacuum spacing from the functionalized GNR edge (Fig. 1a). In contrast, an open boundary condition is imposed at the opposite cell boundary described by a relative permittivity of 1 with the vacuum spacing of 5 Å from the other GNR edge, where the C atom is terminated by the H atom. Fig. 1b shows the schematic diagram of the electrostatic potential for the edge-functionalized GNR under the electric field. We considered the armchair graphene nanoribbon (AGNR) and zigzag graphene nanoribbon (ZGNR), whose edge atomic sites facing the electrode are terminated by O, CHO, COOH, H, OH, and NH functional groups. Fig. 2 shows the optimized geometries of edge-functionalized AGNRs and ZGNRs. To avoid steric hindrance between functional groups on

Table 1: Work functions of AGNRs and ZGNRs with clean and functionalized edges (in eV).

Edge	Clean	O	CHO	COOH	H	NH	OH
AGNR	5.38	7.09	6.21	4.48	3.71	5.95	3.33
ZGNR	6.34	8.12	6.59	4.95	3.84	2.67	1.99

adjacent edge atomic sites for the CHO and COOH cases, the edge atomic sites are alternately terminated by the H atom and the functional group.

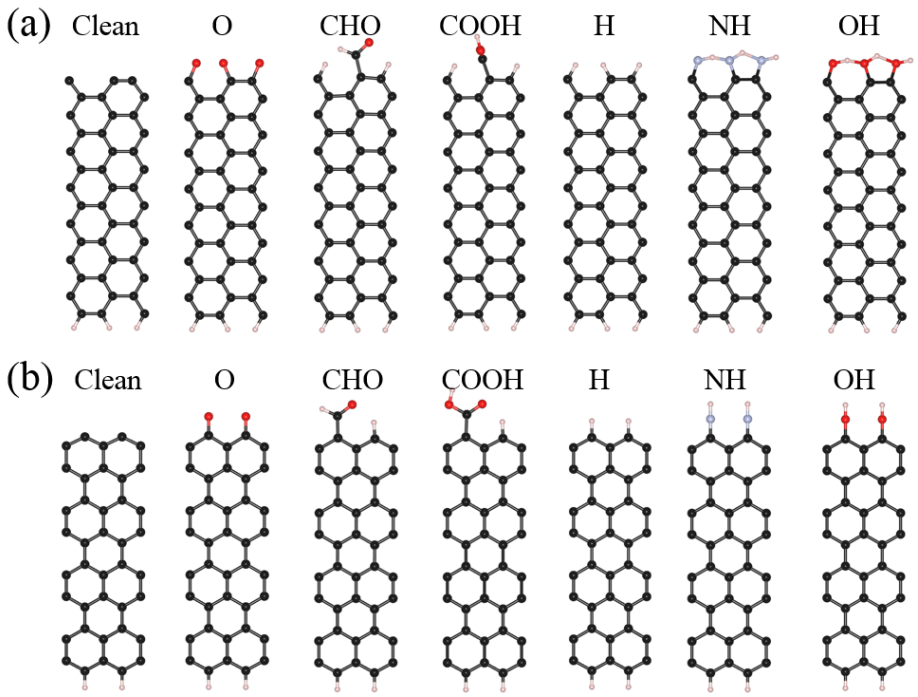

Figure 2: Optimized geometries of functionalized AGNRs and ZGNRs. The C, O, N, and H atoms are colored in black, red, grey, and pink, respectively.

3. Results and discussion

Table 1 shows the work functions of GNRs with clean and functionalized edges with O, CHO, COOH, H, NH, and OH groups. Each work function depends on the attached functional group and edge shape. For the armchair

edge, O, CHO, and NH groups increase the work function to 7.09, 6.21, and 5.95 eV, respectively, from 5.37 eV for the clean edge, while H, OH, and COOH decrease its work function to 3.71, 3.33, and 4.48 eV, respectively. For the zigzag edge, O and CHO groups increase the work function to 8.12 and 6.59 eV, respectively, from 5.95 eV for the clean edge, while H, OH, NH, and COOH functional groups decrease the work function to 3.84, 1.99, 2.67, and 4.95 eV, respectively. The OH group causes the smallest work function for both the armchair and zigzag edges among all functional groups studied here, because it has the largest dipole moment at the edges. The clean zigzag edge has a larger work function than the clean armchair edge [14], so that the work functions of the functionalized zigzag edges are also larger than those of the functionalized armchair edges except when the edge is terminated by OH or NH. For OH and NH functionalization, the zigzag edge shows a smaller work function than that of the armchair edge, because the edge geometries cause the dipole at the zigzag edge functionalized by OH or NH to be stronger than that at the armchair edge.

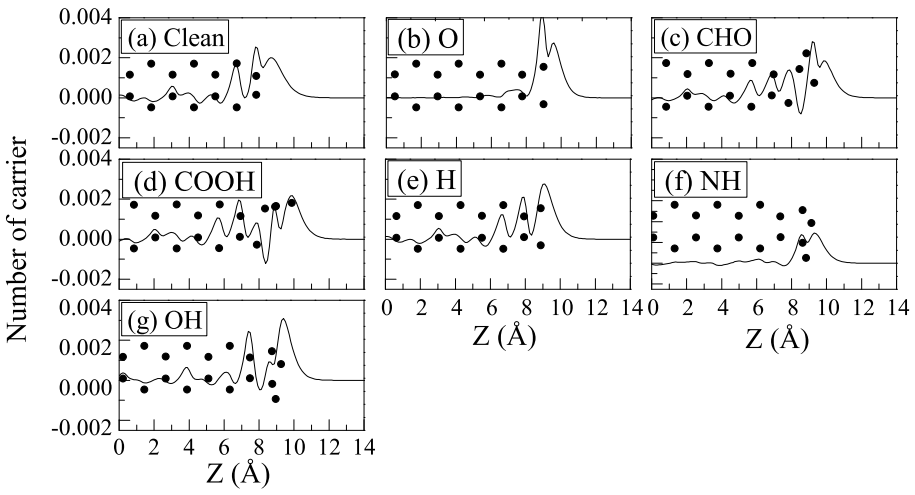

Figure 3: Distribution of accumulated electrons in AGNRs with (a) clean, (b) O, (c) CHO, (d) COOH, (e) H, (f) NH, and (g) OH edges under an external electric field corresponding to doping of 0.05 electrons per unit cell. Black dots in each panel indicate atomic positions.

Figs. 3 and 4 show the distributions of accumulated electrons in AGNRs and

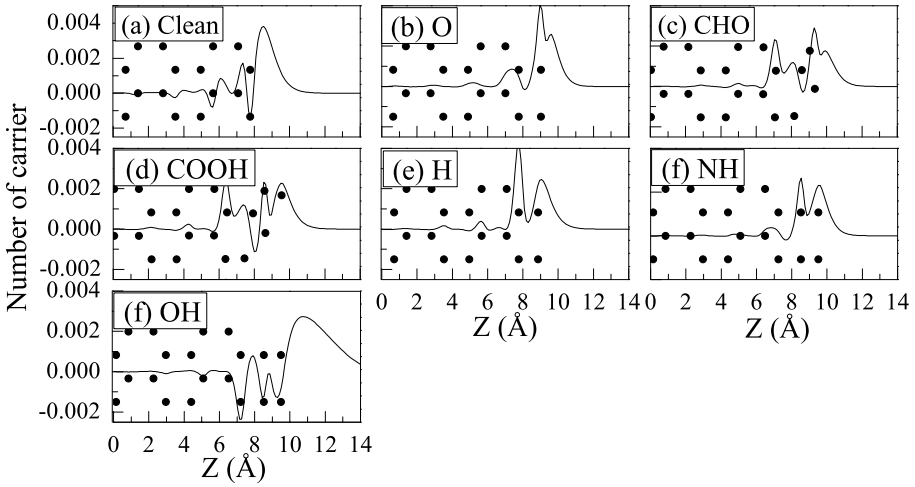

Figure 4: Distribution of accumulated electrons in ZGNRs with (a) clean, (b) O, (c) CHO, (d) COOH, (e) H, (f) NH, and (g) OH edges under an external electric field corresponding to doping of 0.05 electrons per GNR. Black dots in each panel indicate atomic positions.

ZGNRs, respectively, under an external electric field, which injects 0.05 electrons into the GNR. We find that injected electrons are primarily distributed around the ribbon edge depending on the edge shape and functionalization. For the O and NH armchair edges, the carrier concentrations occur near the atomic sites, while for other armchair edges, carriers not only accumulate near the atomic sites but also penetrate inside the GNRs. In contrast, accumulated electrons in GNRs with zigzag edges only penetrate slightly, reflecting the electron distributions around the edges. Electrons are mainly accumulated at functional groups and edge C atoms, suggesting that these atoms contribute to the field emission from the graphene edges. In particular, the electron distributions outside the clean, O, and CHO edges indicate that the dangling bond state at each edge is also responsible for the field emission. By integrating the electron distribution around each edge atomic site, we find that approximately 90% of injected electrons accumulate around the edge atomic sites of all GNRs.

Since the electrostatic potential barrier outside a material is a key factor in determining its field emission, we calculate this barrier for electron emission

from edges with O, CHO, COOH, H, NH, and OH functional groups. Fig. 5 shows the potential barriers of GNRs with clean and functionalized edges as functions of the electric field. Each potential barrier depends on the edge shape and termination. For the armchair edge, the potential barrier decreases monotonically with increasing electric field for all functional groups. Moreover, the potential barrier depends on the edge functionalization: The AGNR with O, NH, or CHO edge has a larger potential barrier than that with a clean edge, while the AGNR with COOH, H, or OH has a smaller potential barrier than that with a clean edge (Fig. 5a). Therefore, we expect that COOH, H, and OH improve the field emission of graphene with armchair edges. In particular, the edge with the OH group will have the largest field emission current among all armchair edges, because it has the lowest external potential barrier among all edge-functionalized AGNRs.

For the zigzag edge, the potential barrier also monotonically decreases with increasing electric field for all functionalizations except for OH, whose potential barrier increases with increasing the field (Fig. 5b). This anomalous property of OH-functionalized ZGNRs with respect to the electric field is attributed to spilled electrons distributed in the vacuum regions and extended alongside the edges, caused by the substantial downward shift of the NFE state crossing the Fermi level [29]. Even when the external electric field increases, the potential barrier of the OH edge remains the lowest for all zigzag edges studied here. As in the case of armchair edges, zigzag edges with O and CHO groups have higher potential barriers compared with other functionalized zigzag edges. Having the lowest potential barrier makes graphene with an OH-functionalized zigzag edge the most efficient for electron emission among the structures studied here.

Finally, we calculated the emission current from functionalized edges as a function of the external electric field. The current density I was calculated from the relation $I = \lambda\nu T$, where λ is the electron density accumulated near the edge by the external electric field, and ν is the collision frequency of electrons estimated by $\nu = E_k/h$ with the electron kinetic energy E_k. The transmission coefficient T is evaluated using the equation $T = \exp\left[\frac{-4\pi}{h}\int\sqrt{2m(V(z)-E_F)}dz\right]$,

where $V(z)$ is the plane-averaged electrostatic potential across the GNRs. Figs. 6a and 6b show calculated emission current densities for the clean and functionalized armchair and zigzag edges, respectively, as functions of the external electric field. Each emission current density I depends on the external electric field, edge shapes, and edge functional groups. Overall, the emission current monotonically increases with increasing electric field. The increase of the current strongly depends on the edge shape and functional group. For the armchair edge (Fig. 6a), an OH, H, or COOH group enhances the emission current, while O, CHO, or NH suppresses the current. The emission current strongly correlates with the potential barrier outside the edge: A small potential barrier leads to a large emission current from the functionalized armchair edges.

For the zigzag edge, the O functionalization substantially suppresses the emission current, while other groups except CHO enhance the current. The NH functionalization provides the largest current because this zigzag edge has a low potential barrier. The zigzag edge with an OH group also has a large emission current because of the low potential barrier outside the edge. Note that the emission current from the OH edge depends less on the external electric field than does that from the other functionalized edges. This implies that the edge with the OH group is stable emission source with respect to the electric field. For H, COOH, CHO, OH, and O groups, the armchair edge provides a larger emission current than that of the zigzag edge, as in the case of clean edges.

4. Conclusion

We used the DFT combined with the ESM method to investigate the electrostatic potential properties of GNRs with zigzag and armchair edges functionalized by O, CHO, COOH, H, NH, and OH groups under an external electric field. Our calculations revealed that the work functions and potential barriers for electron field emission from these edges depend on the attached functional groups. Accordingly, the emission current depends not only on the applied electric field but also on the functional group. GNRs with H, OH, and COOH

functional groups exhibit remarkable field emission currents from their edges, owing to their low potential barriers outside their edges. In contrast, edges with O termination have lower emission currents compared with the other functionalized edges, owing to their higher electrostatic potential barriers outside their edges. The edges functionalized by NH groups show unusual behavior whereby the NH group enhances the field emission current from the zigzag edge but suppresses that from the armchair edge, because the dipole moment of the NH in the zigzag edge is stronger than that in the armchair edge, arising from the conformation difference of NH group.

Acknowledgments

Y. Gao acknowledges the Grant-in-Aid for JSPS Fellows. This work was supported by JST-CREST Grant Numbers JPMJCR1532 and JPMJCR1715 from the Japan Science and Technology Agency, JSPS KAKENHI Grant Numbers JP17H01069, JP16H00898, and JP16H06331 from the Japan Society for the Promotion of Science, and the Joint Research Program on Zero-Emission Energy Research, Institute of Advanced Energy, at Kyoto University. Part of the calculations was performed on an NEC SX-Ace at the Cybermedia Center at Osaka University and on an SGI ICE XA/UV at the Institute of Solid State Physics at The University of Tokyo.

References

[1] J. B. Oostinga, H. B. Heersche, X. Liu, A. F. Morpurgo, L. M. K. Vandersypen, Gate-induced insulating state in bilayer graphene devices, Nat. Mater. 146 (2008) 151–157.

[2] K. I. Bolotin, K. J. Sikes, Z. Jiang, M. Klima, G. Fudenberg, J. Hone, P. Kim, H. L. Stormer, Ultrahigh electron mobility in suspended graphene, Solid State Commun. 146 (2008) 351–355.

[3] Y. Zhang, T. Tang, C. Girit, Z. Hao, M. C. Martin, A. Zettl, M. F. Crommie, Y. R. Shen, F. Wang, Direct observation of a widely tunable bandgap in bilayer graphene, Nature 459 (2009) 820–823.

[4] V. I. Kleshch, D. A. Bandurin, A. S. Orekhov, S. T. Purcell, A. N. Obraztsov, Edge field emission of large-area single layer graphene, Appl. Surf. Sci. 357 (2015) 1967–1974.

[5] A. D. Bartolomeo, F. Giubileo, L. Iemmo, F. Romeo, S. Russo, S. Unal, M. Passacantando, V. Grossi, A. M. Cucolo, Leakage and field emission in side-gate graphene field effect transistors, Appl. Phys. Lett. 109 (2016) 023510.

[6] Z. Xiao, J. She, S. Deng, Z. Tang, Z. Li, J. Lu, N. Xu, Field electron emission characteristics and physical mechanism of individual single-layer graphene, ACS Nano 4 (2010) 6332–6336.

[7] J. T. H. Tsai, T. Y. E. Chu, J. Y. Shiu, C. S. Yang, Field emission from an individual freestanding graphene edge, Small 8 (2012) 3739–3745.

[8] C. Wu, F. Li, Y. Zhang, T. Guo, Field emission from vertical graphene sheets formed by screen-printing technique, Vacuum 94 (2013) 48–52.

[9] A. Malesevic, R. Kemps, A. Vanhulsel, M. P. Chowdhury, A. Volodin, C. V. Haesendonck, Field emission from vertically aligned few-layer graphene, J. Apply. Phys. 104 (2008) 084301.

[10] K. Tada, K. Watanabe, Ab initio study of field emission from graphitic ribbons, Phys. Rev. Lett. 88 (2002) 127601.

[11] M. Araidai, Y. Nakamura, K. Watanabe, Field emission mechanisms of graphitic nanostructures, Phys. Rev. B 70 (2004) 245410.

[12] S. F. Huang, T. C. Leung, B. Li, C. T. Chan, First-principles study of field-emission properties of nanoscale graphite ribbon arrays, Phys. Rev. B 72 (2005) 035449.

[13] Y. Gao, S. Okada, Electrostatic potential barrier for electron emission at graphene edges induced by the nearly free electron states, Appl. Phys. Express 10 (2017) 055104.

[14] Y. Gao, S. Okada, Electrostatic properties of graphene edges for electron emission under an external electric field, Appl. Phys. Lett. 112 (2018) 163105.

[15] T. Kawai, Y. Miyamoto, O. Sugino, Y. Koga, Graphitic ribbons without hydrogen-termination: Electronic structures and stabilities, Phys. Rev. B 62 (2000) R16349(R).

[16] A. Yamanaka, S. Okada, Energetics and electronic structure of graphene nanoribbons under a lateral electric field, Carbon 96 (2016) 351–361.

[17] M. Fujita, K. Wakabayashi, K. Nakada, K. Kusakabe, Peculiar localized state at zigzag graphite edge, J. Phys. Soc. Jpn. 65 (1996) 1920–1923.

[18] K. Nakada, M. Fujita, G. Dresselhaus, M. S. Dresselhaus, Edge state in graphene ribbons: Nanometer size effect and edge shape dependence, Phys. Rev. B 54 (1996) 17954.

[19] Y. Niimi, T. Matsui, H. Kambara, K. Tagami, M. Tsukada, Scanning tunneling microscopy and spectroscopy studies of graphite edges, Appl. Surf. Sci 241 (2005) 43–48.

[20] Y. Kobayashi, K. Fukui, T. Enoki, K. Kusakabe, Y. Kaburagi, Observation of zigzag and armchair edges of graphite using scanning tunneling microscopy and spectroscopy, Phys. Rev. B 71 (2005) 193406.

[21] M. Pan, E. C. Girao, X. Jia, S. Bhaviripudi, Q. Li, J. Kong, V. Meunier, M. S. Dresselhaus, Topographic and spectroscopic characterization of electronic edge states in CVD grown graphene nanoribbons, Nano Lett. 12 (2012) 1928–1933.

[22] X. Zhang, O. V. Yazyev, J. Feng, L. Xie, C. Tao, Y.-C. Chen, L. Jiao, P. Zahra, A. Zettl, S. G. Louie, H. Dai, M. F. Crommie, Experimentally engineering the edge termination of graphene nanoribbons, ACS Nano 7 (2013) 198–202.

[23] L. Talirz, H. Söde, J. Cai, P. Ruffieux, S. Blankenburg, R. Jafaar, R. Berger, X. Feng, K. Müllen, D. Passerone, R. Fasel, C. A. Pignedoli, Termini of bottom-up fabricated graphene nanoribbons, J. Am. Chem. Soc. 135 (2013) 2060–2063.

[24] M. Ziatdinov, S. Fujii, K. Kusakabe, M. Kiguchi, T. Mori, T. Enoki, Visualization of electronic states on atomically smooth graphitic edges with different types of hydrogen termination, Phys. Rev. B 87 (2013) 115427.

[25] M. Posternak, A. Baldereschi, A. J. Freeman, E. Wimmer, M. Weinert, Prediction of electronic interlayer states in graphite and reinterpretation of alkali bands in graphite intercalation compounds, Phys. Rev. Lett. 50 (1983) 761.

[26] M. Posternak, A. Baldereschi, A. J. Freeman, E. Wimmer, Prediction of electronic surface states in layered materials: graphite, Phys. Rev. Lett. 52 (1984) 863.

[27] Q. Liu, Z. Li, J. Yang, Nearly free electron state in graphane nanoribbon superlattice, Chin. J. Chem. Phys. 24 (2011) 22.

[28] A. Yamanaka, S. Okada, Electron injection into nearly free electron states of graphene nanoribbons under a lateral electric field, Appl. Phys. Express 7 (2014) 125103.

[29] R. Taira, S. Okada, Electronic structure modulation of graphene edges by chemical functionalization, Appl. Phys. Express 9 (2016) 115102.

[30] P. Hohenberg, W. Kohn, Inhomogeneous electron gas, Phys. Rev. B 136 (3B) (1964) B864.

[31] W. Kohn, L. J. Sham, Self-consistent equations including exchange and correlation effects, Phys. Rev. 140 (4A) (1965) 1133–1138.

[32] Y. Morikawa, K. Iwata, K. Terakura, Theoretical study of hydrogenation process of formate on clean and Zn deposited Cu (111) surfaces, Appl. Surf. Sci. 169–170 (2001) 11–15.

[33] J. P. Perdew, K. Burke, M. Ernzerhof, Generalized gradient approximation made simple [Phys. Rev. Lett. 77, 3865 (1996)], Phys. Rev. Lett. 78 (7) (1997) 1396.

[34] D. Vanderbilt, Soft self-consistent pseudopotentials in a generalized eigenvalue formalism, Phys. Rev. B 41 (11) (1990) 7892–7895.

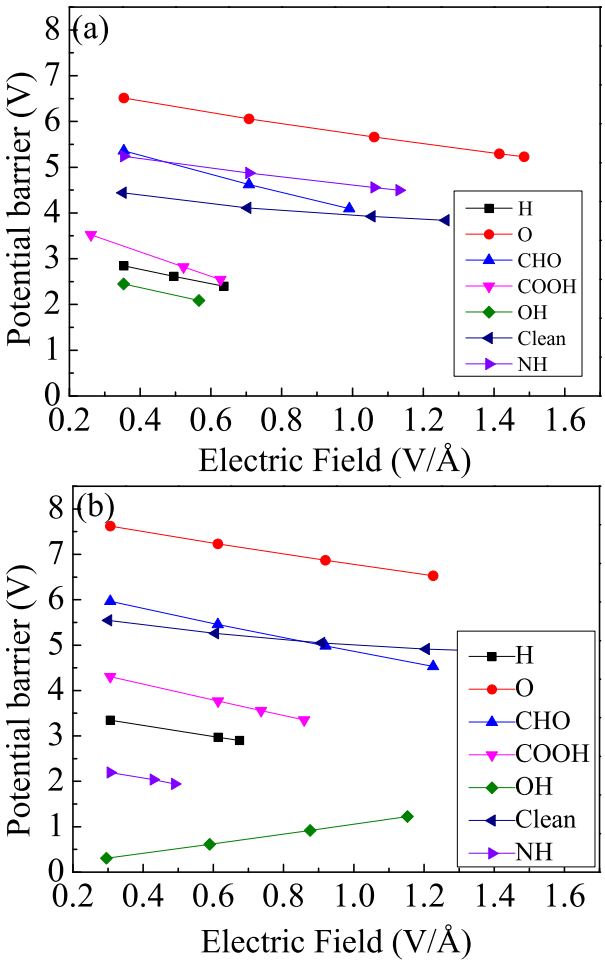

Figure 5: Potential barriers for electron emission from functionalized (a) armchair and (b) zigzag edges as functions of the external electric field.

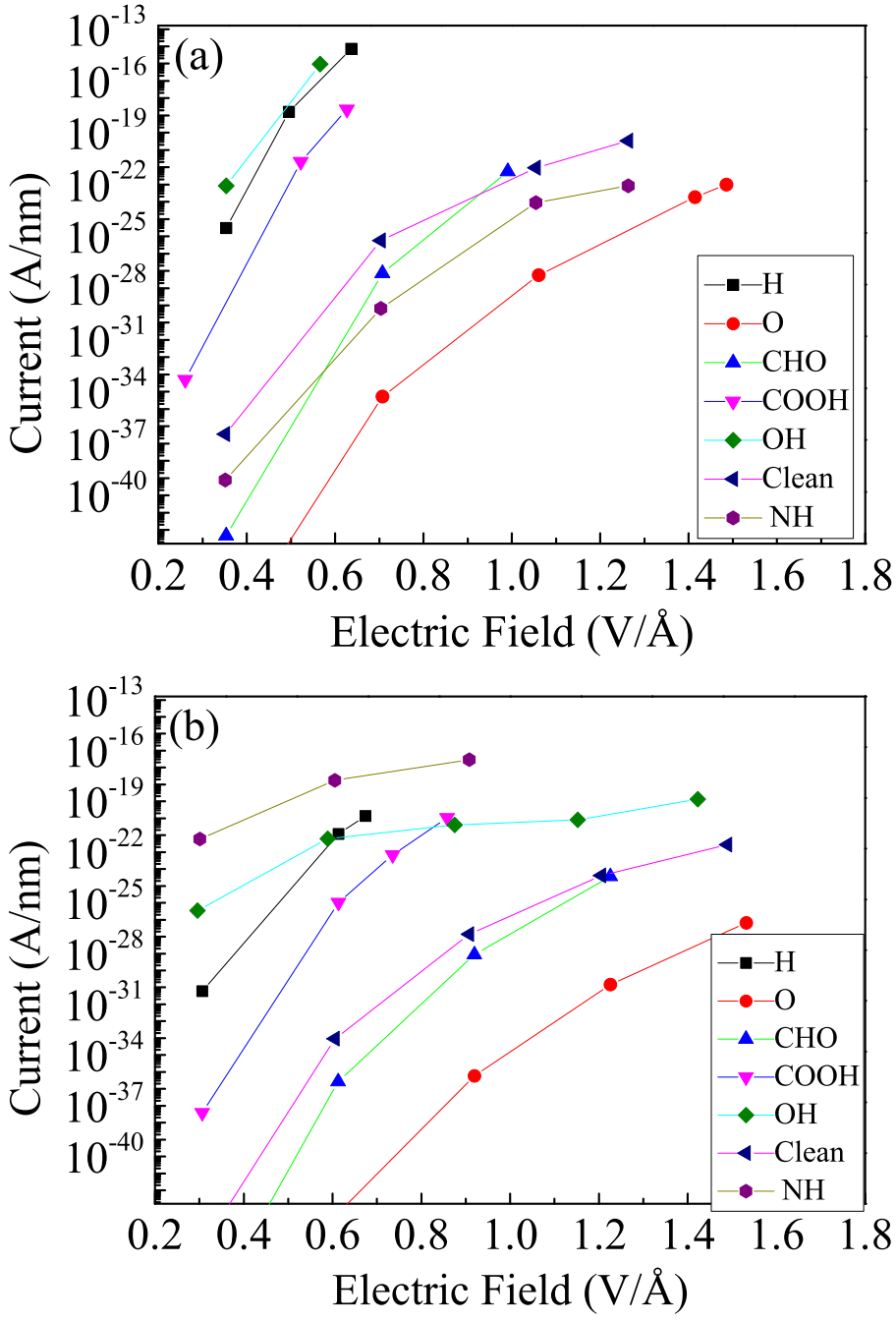

Figure 6: Field emission current densities from functionalized (a) armchair and (b) zigzag edges as functions of the external electric field.